RECENT DEVELOPMENTS IN HIGH INTENSITY ION BEAM PRODUCTION AND PREACCELERATION*

A. van Steenbergen
Brookhaven National Laboratory
Upton, N.Y.

Summary. Some high intensity ion sources, applicable for particle accelerators, are evaluated in terms of extracted beam emittance and source "brightness". Specifically recent results obtained with the duoplasmatron ion source, with and without large plasma expansion cup, are given. It is indicated that a high intensity "rectilinear" ion beam may be obtained from an expanded plasma with a high gradient accelerator structure. Recent approaches to air insulated columns are given, mainly related to the BNL preaccelerator design.

Introduction.

Continuous progress is being made with present particle accelerators to increase the high energy beam intensities. For example, for the BNL AGS, output beam intensities have reached now at least a factor of 10 over that obtained during the early operational period of the accelerator, recent values range up to approximately 1.3×10^{12} particles per pulse. Further plans call for still higher intensities to be achieved by means of a higher AGS injection energy. For this, a new linac injector is being designed. Beam intensities in the injector linac are contemplated to be at least 100 mA of protons. This requires that the preinjector should have the capability of producing a beam output intensity of the order of 300 mA at least. Present developments are directed towards a 500 mA beam intensity preinjector, with output energy of 750 KeV.

For particle accelerators, other than the tandem dc accelerators, the interest centers almost exclusively on proton beams; therefore, negative ion beams and neutral particle beam production[1] will not be discussed here. Also, the discussion here will be limited to a few types of ion sources known to be capable of beam intensities of 100 mA at least, producing simultaneously particle beams with acceptable beam qualities.

In the following first the high intensity ion sources will be discussed, together with the parameters suitable for comparison of the various sources. This will be followed by a discussion of particle beam formation and beam acceleration.

*Work carried out under contract with U.S. Atomic Energy Commission.

High Intensity Ion Sources.

Only recently have ion sources been developed capable of total beam outputs of the order of 500 mA total and being suitable at the same time for use in conjunction with particle accelerators because of beam quality characteristics. A short enumeration of these sources follows. The references cited are pertinent to high intensity operation of the particular source mentioned and are samplings only of the large number of articles dealing with the subject of ion sources.

PIG Ion Source.[2,3]

In this ion source a plasma is obtained by means of a cascade discharge in a structure consisting of a cylindrical or ring type anode with a cathode on either side. A typical configuration is given in Fig. 1a.

In this geometry the electrons oscillate back and forth between the cathodes, their path lengths are increased by means of an axial magnetic field. The electrons lost for the ionization process, because of slow diffusion towards the anode, are replenished by secondary emission from the cold cathodes due to ion impact. High discharge currents may be obtained if the work function for electron emission at the cathodes is reduced. For this reason aluminium is often used for the cold cathodes because of its natural tendency to form aluminium oxide on its surface, thereby reducing the work function. From the point of view of optimum performance it was found to be desirable to use chemically pure aluminium. A typical mass spectrum of the ion beam obtained from the PIG ion source, as used at BNL, is given in Table I.

TABLE I

PIG Ion Source Mass Spectrum

$(m/e)(m/e \text{ for the proton})^{-1}$	Assignment	Relative Abundance
0.55	$H_3^+ \rightarrow H_1^+ + H_2$	< 0.1%
0.69	$H_2^+ \rightarrow H_1^+ + H_1$	< 0.1%
1	H_1^+	60.0%
2.0	H_2^+	8.5%
3.2	H_3^+	1.3%
5.1	O_{16}^{+++}	1%
7.1	(O_{16}^{++})	2.7%

TABLE 1 (Cont'd)

PIG Ion Source Mass Spectrum

(m/e)(m/e for the proton)$^{-1}$	Assignment	Relative Abundance
16	O_{16}^{+}	22%
27	$(A\ell^{+})$	3.3%
∞		$\cong$ 2.2%

Rf Ion Source.[4,5]

In its simplest form this source consists of a discharge chamber in which a rf gas discharge is magnetically excited by means of a coil around the chamber, which is driven either CW or pulsed from a rf oscillator. Frequencies in the range of 1 to 100 Mc/sec are generally employed. Extraction of the ions take place through a narrow cylindrical canal, either by the diffusion of the ions through the canal or by introducing an extra electrode in the chamber, which is given a (usually pulsed) positive potential; in this case the ions leave the source with a higher energy. This extra electrode may be pulsed up to 50 kV and the ions leave the source with this equivalent energy. An example of this ion source, as used at CERN[5], is shown in Fig. 1b. To counteract recombination the extraction channel is covered with a ceramic or pyrex cover.

Duoplasmatron Source.[6,7,8]

Between cathode and anode of a hot cathode two electrode discharge geometry, a conical intermediate electrode is inserted which serves to compress the plasma. Further compaction, between the intermediate electrode and anode is accomplished by means of a magnetic mirror field for the electrons around the interspace of these electrodes. More precisely, in the part of the intermediate electrode closest to the anode the mirror field becomes active and the plasma is contracted away from the walls, which effectively decreases recombination. The electrons lost from the plasma are replenished by electrons from the hot cathode. Having lost their initial energy in the ionization process, these electrons are further accelerated toward the intermediate electrode channel through one or more plasma double layers, producing as a consequence a high plasma density in the front part of the intermediate electrode. This is then further compacted by the mirror fields. For higher output currents, a specially shaped aperture button makes it possible to obtain ion emission from a larger area than the source aperture opening (small plasma expansion cup). Schematically the source is illustrated in Fig. 1c, and a mass spectrum obtained with the BNL duoplasmatron is given in Fig. 2.

Lamb-Lofgren Ion Source.[9]

This source is a version of the "Magnetic" ion source i.e., the hot cathode discharge type source with plasma concentration by means of an axial magnetic field. Here, instead of a single aperture hole, a multiple of apertures is used to let the plasma expand in a large cylindrical plasma expansion cup. With the extraction field a concave plasma sheath is formed within the relatively large plasma expansion cup. Plasma boundary shaping ("plasma boundary focussing") may thus be obtained either with the shape of the multiple holed boundary structure or with the shaping of the extraction field.

"Modified" Duoplasmatron Source.[10]

A large plasma extraction cup is attached to the basic duoplasmatron source and ion extraction takes place from a shaped plasma boundary sheath. A version of this type presently being studied at BNL is shown in Fig. 3. As indicated there the plasma boundary shaping may be obtained with a fine mess tungsten grid.

"Modified" PIG Source.[11]

This ion source incorporates the basic PIG source together with a hot cathode and a large plasma expansion cup.

Some pertinent parameters of the ion sources mentioned above have been collected from the literature and from BNL experience. These are listed in Table II. The figures given are meant for comparison and should be considered to be approximate only. It is evident from the values cited that ion sources using plasma expansion and plasma boundary focussing are capable of producing the desired beam intensities of the order of 500 mA. Actually, it is in a sense secondary how the expanded plasma is established, as long as the appropriate plasma temperature and density may be obtained. Therefore, in a first approach several of the mentioned ion sources will be suitable and there should be no clear-cut choice between the "modified" PIG source, the Lamb-Lofgren "Magnetic" source and the "modified" duoplasmatron source. However, with the duoplasmatron, a high density primary plasma is obtained in a rather efficient way. This source is, therefore, more suitable to produce an expanded plasma without actually enlarging the ion source aperture to any appreciable extent. This is desirable in connection with neutral gas flow in the acceleration column when operating this source in a pulsed fashion.

TABLE II

Evaluation of High Intensity Ion Sources

Reported maximum	Units	PIG Source	Rf Source	Duo-plasmatron Source	With large plasma expansion and plasma boundary focusing: Lamb-Lofgren "Magnetic" Source	PIG Source With Hot Cathode	Modified Duoplasmatron Source
Ion currents:							
after single electrode acceleration	mA	150	350	1000	1000	1000	800
after C-W acceleration	mA	90	250	150	____	____	400
Physical characteristics:							
beam energy spread	ev	<10	10	<1	____	____	____
typ.max.proton perc.	%	50-80	60-90	60-90	95	____	____
Characteristics: gas consumption	Nm^3/h	10-100	10-100	50	2000	1000	100-200
related to complexity of auxiliary equipment: (power input* / duty factor)	kw	0.5-5	1-10	0.5-2	5-10	5	1-5
power for solenoids etc.	kw	1	0.5	0.5	10	1	0.5
cathode heating	kw	____	____	0.1-0.5	1	0.1-0.5	0.1-0.5
discharge current	A	1-5	____	10-40	100	40	20-100

*Related to source discharge current only.

Emittance and Ion Source Brightness.

To establish further criteria by which to judge the performance of the various ion sources it is useful to define beam emittance again and related to this source "brightness". Consider the particle density in six dimensional phase space. This, for the particle beams under consideration, may be simplified to the particles per unit time density in the four dimensional transverse phase space projection, assuming a simplified E, t distribution. The source brightness or beam brightness for a definite particle energy is now defined as

$$B_4 = \frac{I}{V_4(x,y,x',y')}$$ where I is the total ion current, V_4 is the four dimensional volume,

$$x' = \frac{dx}{dz} = \frac{p_x}{p_z} \quad \text{and} \quad y' = \frac{dy}{dz} = \frac{p_y}{p_z} .$$

This definition is analogous (but not identical) to the statement that the source brightness is the particle flux (current density) per unit solid angle (see below).

Because of the density conservation in phase space in accordance with Liouville's theorem,* for a lossless beam transport system, the invariant

$$\mathfrak{B}_4 = \frac{I}{\beta^2\gamma^2 V_4}$$

may be obtained, i.e. the momentum normalized density in four dimensional transverse phase space. Here β and γ have the usual meaning, i.e. $p_z = m_o c \beta\gamma$.

For a "normal" beam, that is, for an axial symmetric beam, for which the intercepts of the four dimensional volume with both transverse phase planes are identical ellipses, it has been shown by Walsh [12,13] that:

$$V_4 = \frac{1}{2}(A_2) \quad \text{and} \quad \mathcal{E}_4 = \frac{\beta^2\gamma^2 V_4}{(\pi^2/2)}$$

*Transverse and longitudinal motion is assumed to be uncoupled.

where A_2 is the two dimensional phase space area and $\mathcal{E}_4$ is the four dimensional momentum normalized emittance. With the usual definition of two dimensional momentum normalized emittance:

$$\mathcal{E}_2 = \frac{\beta\gamma A_2}{\pi} \qquad \text{it follows that}$$

$$\mathcal{E}_4 = (\mathcal{E}_2)^2 \qquad \text{and consequently}$$

$$\mathcal{B}_4 = \frac{I}{\frac{\pi^2}{2}(\mathcal{E}_2)^2}$$

The usefulness of this definition stems from the fact that in general the maximum beam intensity transport in an accelerator sub-component is determined by $\mathcal{B}_4$ of the preceding source, in the present case the ion source, whereas in practice normally only the two dimensional emittance $\mathcal{E}_2$ has been measured.

The relation between source brightness or beam brightness and two dimensional emittance, as given here, refers strictly speaking to "normal" beams only. In practice two dimensional phase space boundaries are encountered which diverge sometimes greatly from elliptical boundaries. Nevertheless, the same definition for $\mathcal{B}_4$ as related to $\mathcal{E}_2$ will be used, i.e. for non-axial symmetric beams the beam brightness is defined as [14]:

$$\mathcal{B}_4 = \frac{I}{\frac{\pi^2}{2}(\mathcal{E}_2)_{x,x'}(\mathcal{E}_2)_{y,y'}} = \frac{I}{(\frac{1}{2})(\beta\gamma)^2 (A_2)_{x,x'}(A_2)_{y,y'}}$$

Experimental Observations

Extensive measurements of phase space area and density distribution have been done with the duoplasmatron source at an energy level of 750 KeV.[15] Also some results were obtained with the PIG source. A typical two-dimensional distribution for the PIG source is shown in Fig. 4. Similarly for the duoplasmatron, the results are shown in Fig. 5, which is to be compared with the emittance boundaries obtained by measuring directly within the duoplasmatron extraction electrode at energy levels around 50 KeV, as shown in Fig. 6. The low energy measurements were done by L. Oleksiuk, who also obtained the preliminary results with the "modified" duoplasmatron source, as shown in Fig. 7. Here, a plasma expansion cup of 1-in. diameter was used. In one case, Fig. 7a, a fine tungsten mesh was used on the extraction electrode and a total beam intensity of approx. 700 mA was measured with a current transformer in the extraction electrode.

The performance of the rf ion source has been improved greatly by the CERN PS group; with this source ion currents of the order of 200 mA have been obtained and beam emittance measurements have been reported by Sluyters.[16]

Referring now to the conventional duoplasmatron source, the rf source and the PIG source only, it was found that for these ion sources the source brightness or beam brightness decreased linearly with the output beam intensity or the two dimensional emittance values increased linearly with output beam intensity. This behavior is expressed as:

$$\mathcal{B}_4 = \frac{2(\delta_2)^2}{I} \qquad \text{and}$$

$$\mathcal{E}_2 = \frac{I}{\pi\delta_2} \qquad \text{with } \delta_2 \text{ a constant.}$$

Here, δ_2 is the normalized "density" in two dimensional phase space,

$$\delta_2 = \frac{d_2}{\beta\gamma} \qquad \text{and} \qquad d_2 = \left(\frac{A_2}{I}\right)^{-1}, \quad \text{the}$$

"density" in the two dimensional (x,x') phase space projection.* The results for the three mentioned sources are plotted in Fig. 8, where A_2 is given as a function of total beam output. Two distinct regions are observed referring to emittance results obtained immediately after the source or after acceleration in a preaccelerator column. This indicates a loss of "density" in the two-dimensional phase space distribution or equivalently a loss of beam brightness in the transport from the 50 KeV level to the 750 KeV level. The results shown in Fig. 8 were normalized and the brightness values were determined. This is summarized in Fig. 9 where the invariants $\mathcal{E}_2$ and $\mathcal{B}_4$ are given. Preliminary results obtained with the modified duoplasmatron source by L. Oleksiuk at BNL and B. Vosicki[17] at CERN indicate somewhat higher brightness values at output currents of the order of 400 mA than an extrapolation of the present results would indicate.

Source Brightness Related to T_i, T_e of the Plasma.

As indicated by the foregoing results it is apparent that the same behavior is observed for either of the ion sources discussed here. The question arises to what extend the ion source and the state and geometry of its plasma is responsible for the observed beam brightness and measured emittance values, and the rather unpleasant behavior that the four dimensional phase space density decreases when higher beam intensities are obtained from these ion sources.

Therefore, consider a plain plasma boundary. The distribution of transverse momenta is only

* It is not implied here that a homogeneous density distribution is present, and δ_2 and d_2 should be regarded as average values only.

due to the ion temperature near the plasma boundary (sheath). Assuming now the simplest case of ion extraction from a plasma area πR^2, a homogeneous density filling of the plasma of N ions/unit volume and a stable plasma sheath, then the four dimensional phase volume is given by

$$V_4 = \int dxdydx'dy' \quad \text{with} \quad x' = p_x/p_z$$

and $y' = p_y/p_z$ and p_z a constant.

Because x' and y' are dependent on the ion temperature only, i.e. independent of the x and y values, it follows after conversion to cylindrical coordinates that V_4 is given by:

$$V_4 = \int_0^R \int_0^{2\pi} RdRd\theta \int_0^{p_t(max)/p_z} \int_0^{2\pi} pdpd\beta$$

whereby the second integral integrates over all possible p vectors within the solid angle centered at $R=R, \theta=\theta$. This integrated yields:

$$V_4 = \pi^2 R^2 \left(\frac{p_t\ (max)}{p_z}\right)^2$$

An expression for the value of the maximum transverse momenta present at the plasma sheath may be obtained from the Maxwell-Boltzmann velocity distribution by assuming a simple cut-off value at twice the rms velocity. Graphical integration shows then that more than 90% of the total number of particles is being included, which is sufficient for the present argument. From this:

$$p_t(max)/p_z = \frac{2\sqrt{km_o T_i}}{(m_o \gamma\beta c)} \quad \text{where}$$

T_i is the ion temperature. Consequently

$$V_4 = \frac{4\pi^2 R^2 (km_o T_i)}{(m_o c\beta\gamma)^2}$$

With the normalized source brightness or particle density in the four dimensional transverse phase space defined as before, it follows that

$$\mathcal{B}_4 = \frac{I}{4\pi^2 R^2} \left(\frac{k\ T_i}{m_o c^2}\right)^{-1}$$

For a stable plasma sheath the Bohm "criterium"[18] demands that ions reach the sheath with a velocity given by:

$$v_z \geq \left(\frac{k\ T_e}{m_o}\right)^{\frac{1}{2}}$$ where T_e is the electron temperature of the plasma electrons. With an applied field the sheath potential fall would add to this value and for practical cases ($\cong$ 5 Volts) v_z would be approximately larger by a factor of 2. From this, with the diffusion equation:

$I = 2\pi R^2\ Ne \left(\frac{k\ T_e}{m_o c^2}\right)^{\frac{1}{2}}$. This substituted in the expression for $\mathcal{B}_4$ yields:*

$$\mathcal{B}_4 = \frac{Nec}{2\pi} \left(\frac{m_o c^2}{k\ T_i}\right)^{\frac{1}{2}} \left(\frac{T_e}{T_i}\right)^{\frac{1}{2}}$$

It should be realized that the assumed transverse momentum distribution is not analogous to that present in a "normal" beam, as defined before, and the relationship

$$\mathcal{B}_4 = \frac{I}{(\pi^2/2)(\varepsilon_2)^2}$$ is not necessarily valid.

For the case at hand, i.e, the intercepts with the two dimensional phase planes are rectangles, instead of ellipses, one obtains* $\mathcal{B}_4 = I\ (\pi\varepsilon_2)^{-2}$. Consequently, with this

$$\varepsilon_2 = \left(\frac{2}{\pi}\right)^{\frac{1}{2}} \frac{I^{\frac{1}{2}}}{(Nec)^{\frac{1}{2}}} \left(\frac{k\ T_i}{m_o c^2}\right)^{\frac{1}{4}} \left(\frac{T_i}{T_e}\right)^{\frac{1}{4}} = 2R\left(\frac{k\ T_i}{m_o c^2}\right)^{\frac{1}{2}}$$

As is indicated by the expression for $\mathcal{B}_4$, if the T_e and T_i values are in a first approach independent of N, and a fixed plasma boundary area is assumed then

$$\mathcal{B}_4 = C_1 N = C_2 I.$$

Actually, because of limitations in beam extraction due to space charge effects a more practical expression than, I = const. $\pi R^2 N$ is given by Langmuirs equation.

$$I = C\pi R^2 \frac{V_{extr.}^{3/2}}{g^2}.$$

*For the "rectangle distribution" beam assumed in the present case:

Comparison of $V_4 = \pi^2 R^2\ (p_t^{(max)}/p_z)^2$ with $A_2 = 4R\ (p_t^{(max)}/p_z)$, i.e. the two dimensional distribution obtained at the plasma boundary, it follows that

$V_4 = (\frac{\pi}{4})^2 (A_2)^2$. To be consistent it is necessary to redefine the two dimensional emittance here, $\varepsilon_2 = \beta\gamma \frac{A_2}{4}$. Consequently $\mathcal{B}_4 = \frac{I}{\beta^2\gamma^2 V_4} = \frac{I}{\pi^2 \varepsilon_2^2}$.

Comparison of the two expressions indicates that a practical upper limit exists for N (N_{opt}) given by the maximum value of

$$\left(\frac{V_{extr}}{g^2}\right)^{3/2}.$$

For higher values of N and given extraction field and geometry the plasma boundary takes on such a shape that inacceptable optical conditions result. Therefore, for any practical system, the maximum value of N may not be determined by the ion source capabilities only, but, especially with recent source developments, by limitations in

$$\left(\frac{V_{extr}}{g^2}\right)^{3/2}.$$

Substitution of I given by Langmuirs equation in the expression for $\mathfrak{B}_4$ yields:

$$\mathfrak{B}_4 = \frac{C}{4\pi}\,\frac{V_{extr}}{g^2}^{3/2}\left(\frac{k\,T_i}{m_o c^2}\right)^{-1} \quad \text{or, in this case,}$$

$\mathfrak{B}_4$ = Const. Also, here, $N=N_{opt}$ and the total current can only be increased by increasing πR^2. For a value of $V_{extr.} = 50$ kV and $g_{eff}=0.5$cm, one obtains $I/\pi R^2 \cong 2$ A/cm^2 and $N_{opt} \cong 10^{12}/cm^3$.

Also, referring to experimental results obtained at BNL,[15] for the particular geometry used with the conventional duoplasmatron source and values at

$$\left(\frac{V_{extr}}{g^2}\right)^{3/2},$$

the maximum current density of $I/\pi R^2 \cong 2$ A/cm^2 was reached at a total current of I = 10 mA and larger currents were only obtained by letting the plasma expand to a certain extent and extracting from a boundary area several times the area of the source aperture. Even though this value of 10 mA depends directly on

$$\left(\frac{V_{extr}}{g^2}\right)^{3/2},$$

of which the optimum value would vary for various practical systems, it is assumed here that the transition from the low current to the high current regime would occur at approximately this value.

In summary, the expected behavior of emittance and source brightness as a function of total current, if dependent on T_i, T_e of the plasma only, is given by:

$N < N_{opt}$	$N = N_{opt}$
$\varepsilon_2 = C^o$	$\varepsilon_2 = C^{oo} I^{\frac{1}{2}}$
$\mathfrak{B}_4 = C_o I$	$\mathfrak{B}_4 = C_{oo}$
(I < 10mA)	(I > 10mA)

Comparison with Experimental Results

The inverse proportionality of $\mathfrak{B}_4$ with I has been indicated before.[6] Further, substituting some typical values for N, T_i, T_e in the calculated expression for $\mathfrak{B}_4$, i.e.

$n_i \cong n_e \cong 10^{12}/cm^3 = N$, $T_e \cong 3\ 10^5\ ^oK$, $T_i \cong 3\ 10^3\ ^oK$ one finds $\mathfrak{B}_4 \cong 4.10^{11}$ mA/cm^{2}rad^2.

Comparing this and the expected current dependence with the experimentally observed behavior, i.e. extrapolating experimental values to the regions of output currents of the order of 1 mA, a value of $\mathfrak{B}_4$ (exp.) $\cong 4\ 10^9$ is observed; it is clear that experimental observed emittance values and source brightness values are not related in a first approach to T_i, T_e of the plasma. The actual observed values are either due to effective enlargement of the distribution in transverse momenta due to aberrations,* present in any practical system, or due to plasma boundary instabilities[19] such that time dependent boundary instabilities exist of which the time average value is measured. Probably both effects are present. Actually, the pronounced behavior that $\mathfrak{B}_4$ varies inversely with I_{tot} suggest an effective enlargement of the beam emittance related to space charges effects. This could be due to spherical aberrations specifically introduced as a consequence of space charges forces in the beam, i.e. the potential difference between paraxial and peripheral ions result in a loss of homogeneity in the beam. Especially, in the extraction region this effect could be pronounced at higher beam intensities. The loss of homogeneity of the beam, or the variation of current density with the transverse coordinate r leads to a beam expansion depending on the magnitude of r and hence aberrations.

For completeness sake it seems useful to compare the source brightness as defined here with the "richtstrahlwert", R_i, as used for electron beams and applied to ion beams by Von Ardenne.[6] R_i is defined as the current density per unit solid angle at a beam cross over or "waist".

*In an axial symmetric system, with no solenoidal components present, this would effectively enlarge the p_r distribution, but not the p_θ distribution.

The relationship

$$\mathfrak{B}_4 = \left(\frac{1}{\beta^2\alpha^2}\right)\left(\frac{2}{f^2}\right) R_i \quad \text{holds, whereby., } 0<f<1.^*$$

Evaluation of some BNL results indicated for a particular case a value of $f \cong 1/10$. Actually the R_i value is measured at a beam cross-over by determining cross-over radius and maximum inscribed cone of the beam. This depends on the behavior of the beam periphery, which is sensitive to current density in the beam. The behavior of the beam periphery for a beam with a certain emittance value and with the influence of space charge forces has been derived by Walsh[13] and the results are relevant here.

Further Developments

As is clear from the foregoing from the point of view of source brightness there is no preference for either of the expanded plasma sources mentioned here, and for reasons given before the modified duoplasmatron source seems most suited for obtaining high output proton beam intensities. However, it is not so that one could speak of an operational source at the present time. Further developments are needed. Some problems are mentioned:

1. With the large plasma boundary extraction, use is made of plasma boundary focusing, i.e. the beam optics will depend on the plasma boundary shape. This in turn depends sensitively on extraction field, its distribution and plasma density. Slight variations in source parameters are expected to affect beam optics substantially. In this connection also the non-uniform plasma density is a problem resulting in complex emittance patterns. For plasma boundary shaping a grid might be used, as was shown in Fig. 3. If a grid is used on the extraction electrode scattering of protons due to the fine structure of the local fields might prove to be causing effective dilution of phase space. Preliminary results obtained at BNL by A. Oleksiuk seems to indicate that this is not of any appreciable magnitude.

2. Plasma oscillations and boundary instabilities. With the conventional duoplasmatron source, beam intensity modulations with frequencies up to 30 Mc/sec and even higher, have been observed with the wide-band frequency system of the Alternating Gradient Synchrotron. At times, beam intensity modulations of nearly 75% have been observed, while under optimum conditions this was still of the order of 5% to 10%. Presently, this problem is being studied at BNL by Th. Sluyters with the modified duoplasmatron source. Preliminary results indicate that some geometry changes in the source were quite effective in reducing intensity modulations while maintaining a high current capability.

3. Further measurements are needed on proton percentage from an expanded plasma from the modified duoplasmatron source, because of the expected lower ion temperatures near the plasma boundary, which could affect proton percentage.

*It is expected that for an aberration free system and no space charge blow-up effects present $f \rightarrow 1$.

Beam Formation and Acceleration

Regarding the problem of beam formation, beam transport between ion source and accelerator column and acceleration in the preaccelerator, it is necessary to take into account, especially at the higher beam intensities encountered in recent preaccelerator facilities, the beam blowup due to space charge forces. Here, use is normally made of Poisson's equation, which for an axial symmetric beam, with homogeneous density distribution, for the case of non-relativistic particles, and paraxial motion, yields the well known equation:

$$Vr'' + \frac{V'r'}{2} + \frac{V''r}{4} + \frac{CI}{rV^{\frac{1}{2}}} = 0$$

Typically, at BNL, this equation has been numerically integrated with $V' = \text{Const.}$ and $V'' = 0$, to obtain the orbits in the 750 KeV accelerator column.

This equation is valid for the paraxial case only and with the stated restrictions. Typically, terms in $(r')^2$ and higher order terms are assumed to be zero. For cases where the large beam intensity demands large R and dR/dZ values at the entrance of the accelerator column, the validity of the paraxial equation for the design of the optical system between ion source and accelerator column becomes doubtful. Also, it has been assumed that the beam emittance is zero. Referring to beam periphery only an extra term $(C\varepsilon^2/r^3)$ is added on the left-hand side of the above equation if a "normal" beam is considered with finite emittance value[13]. In this respect also the work of Kirstein[20] should be mentioned, where, for example, the introduction of non-linear components in the space charge field because of the current density distribution in a beam with finite emittance, is discussed. Recently, relaxation programs[21] have been developed to obtain solutions of Poisson's equations without the usual approximations. Another approach used by Pierce[23] for zero emittance beams is to keep r constant (for cylindrical beams typically) and to enforce at the beam boundary the potential distribution obtained from the above paraxial equation with $r' = r'' = 0$. With non-zero emittance the paraxial equation reduces in this case to:

$$\frac{V''r}{4} + \frac{C'I}{rV^{\frac{1}{2}}} + \frac{C''\varepsilon^2}{r^3} = 0 \quad \text{where here again r}$$

refers to the beam periphery only.

Actually, with the possibility of extracting ion beams from larger plasma boundary diameters it becomes worthwhile to consider again the Pierce approach. For small beam diameters in the extraction region with current densities of the order of 1 A/cm^2 inpracticable high gradients are required to enforce a "rectilinear" beam. With the modified duoplasmatron source, with current densities of the order of 0.1 A/cm^2 the required fields approach practical values again.

For a total beam current of 500 mA, and in the approximation of zero emittance values, the potential distribution has been obtained from the paraxial equation. This result has been used to obtain a first design for a practical system to transport and accelerate 500 mA of protons. It is intended to refine the approach by using the Kirstein-Hornsby program[21] and by integration of the paraxial equation with finite emittance value, as given above.

For the rectilinear flow with cylindrical boundaries the axial distribution is given by:

$$U_{z,o} = A_i z^{4/3} \quad \text{with}$$

$$A_i = \left(\frac{m_p}{m_e}\right)^{1/3} A_e \quad \text{and} \quad A_e = 5.7\ 10^3\ j^{2/3}$$

For a plasma boundary of 1 in. diameter and I_{tot} = 500 mA it follows: j = 0.1 A/cm^2 and $U_{z,o} = 1.5\ 10^4\ z^{4/3}$.

The potential distribution outside the beam boundary has to match the distribution at the beam boundary. This has been obtained analytically and can be approached for practical electrode shapes with an electrolytic tank. The axial distribution together with the required fields as a function of axial location is given in Fig. 10. In this case the extraction electrode held at 50 kV is matched at the proper location and given the appropriate shape. Consequently 700 kV will be held across a gap of approximately 16.5 cm. The maximum axial field indicated is approx. 50 kV/cm. Similarly some parameters for the spherical case, i.e. a beam cone cut out of the inner space between two spheres has been explored. Again, a plasma boundary diameter of 1 in. and total beam of 500 mA have been assumed. The axial potential distribution is also given in Fig. 10. The field has been limited to 10 MV/m, resulting in this case in a slight deviation from the required potential distribution above 650 kV. This is not thought to be serious. As a first approach the rectilinear beam with cylindrical beam boundaries have been considered and the electrode system enforcing the required potential distribution has been designed. Electrode shapes and equipotential distributions were obtained by A. Soukas, BNL, who also constructed a 30 in. x 24 in. electrolytic tank with semi-automatic potential plotter. A typical potential plot is given in Fig. 11. The indicated electrode structure will be mounted in a high gradient large diameter column structure, as shown in Fig. 12. This is a double-walled structure with the possibility of conditioned and cooled gas mixture flow in the interspace for cooling of the voltage dividing resistors and improved voltage rating. The total length of the column is about 40 in. for 750 kV. A 3-electrode prototype section has been built to evaluate some of the design approaches in more detail and testing of this 300 kV section has just started.

Acknowledgement

In addition to the contributions by Th. Sluyters and A. Soukas, already mentioned in the foregoing, I want to acknowledge the assistance of V. Buchanan, responsible for the mechanical design of the accelerator column and of R. Damm, who executed the mechanical design of the ion sources and constructed the special high gradient column dividing resistors.

References

1) P.H. Rose, Nuclear Instr. and Methods 28, 1964, 146.
2) J. Flinta, Nuclear Instr. 2, 1958, 219.
3) R. Pauli, J. Flinta, Nuclear Instr. 2, 1958, 227.
4) T. Harrison, P.C. Thoneman, A.E.R.E. Report GP/R1190.
5) C.S. Taylor "Proc. Dubna Accelerator Conf. 1963", 475 (Atomizdat 1964).
6) M. von Ardenne, "Tabellen der Elektronen Ionenphysik und Ubermikroskopie", VEB Deutscher Verlag der Wissenschaften, Berlin 1956.
7) R.A. Demirkhanov, O.F. Poroshin, P.E. Bielensov, G.P. Mkheidze, "A Collection of High Energy Accelerator Papers from U.S.S.R." BNL Report 767 (C-36), 1962, 218
8) R.A. Demirkhanov, H. Freulich, U.V. Kursanov, T.I. Gutkin, Ibid., 224.
9) W.A.S. Lamb, E.J. Lofgren, R.S.I. 27, 1956, 907.
10) M.A. Abroyan, V.P. Gerasimov, F.G. Zheleznikov, G.R. Zablotskaja, N.F. Ivanov, A.V. Ivlev, V.L. Komarov, V.S. Kuznetsov, G.M. Latmanizova, I.M. Royfe, A.I. Solnyshkov; "Proc. Dubna Accelerator Conf., 1963", 507 (Atomizdat 1964)
11) M.D. Gabovich, L.L. Pasechnik, L.I. Romanyuk, Z. Tek. Fiz. 31, 1961, 87.
12) T.R. Walsh, J. Nuclear Energy, Part C. 4, 1962, 53.
13) T.R. Walsh, J. Nuclear Energy, Part C, 5, 1963, 17.
14) A. van Steenbergen, L.W. Oleksiuk, J.P. Blewett, " Proc. Dubna Accelerator Conf. 1963", 489 (Atomizdat 1964).

15) A. van Steenbergen, "Conf. on Linear Accelerators, 1962", BNL6511, 338.
16) Th. Sluyters, CERN MPS/Int 1963, LIN 63-6.
17) B. Vosicki, CERN, private communication.
18) A. Guthrie, R.W. Wakerling, "The Characteristics of Electrical Discharges in Magnetic Fields". McGraw-Hill, May 1949.
19) H. Wroe, AERE, private communication.
20) P.T. Kirstein, Joint Institute of Nuclear Research, Dubna, U.S.S.R., preprint, E-1033.
21) P.T. Kirstein, J.S. Hornsby, CERN, AR Div. Report 63-16, 1963.
22) A.I. Solnyshkov, Yefremov Institute, Leningrad, private communication
23) J.R. Pierce, "Theory and Design of Electron Beams", 2 ed. D. van Nostraud Co., N.Y. 1954.
24) L.W. Oleksiuk "Conf. on Linear Accelerators, 1964" MURA, UC-28.
25) U. Talgren CERN MPS/Int Lin. 62-3

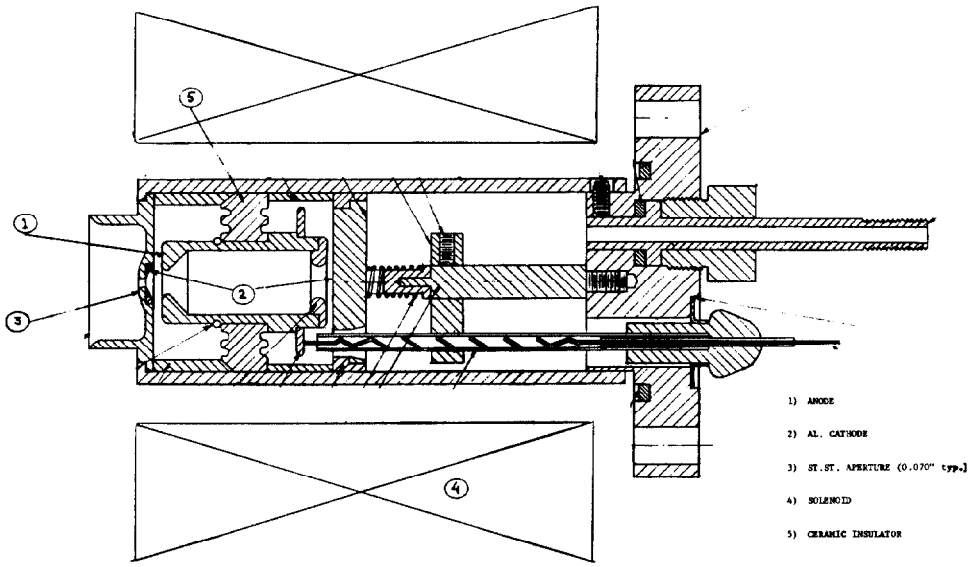

P. I. G. ION SOURCE

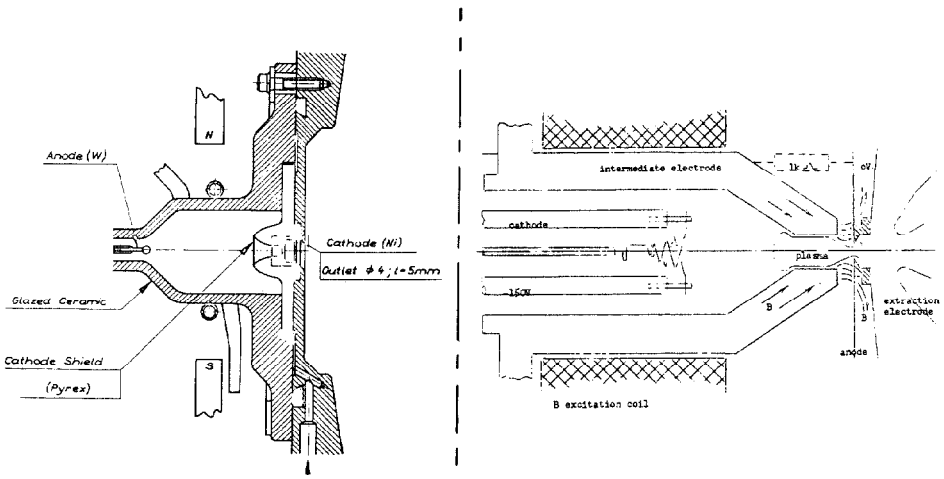

RF ION SOURCE (REF. 5) DUOPLASMATRON

Fig. 1. Various ion sources.

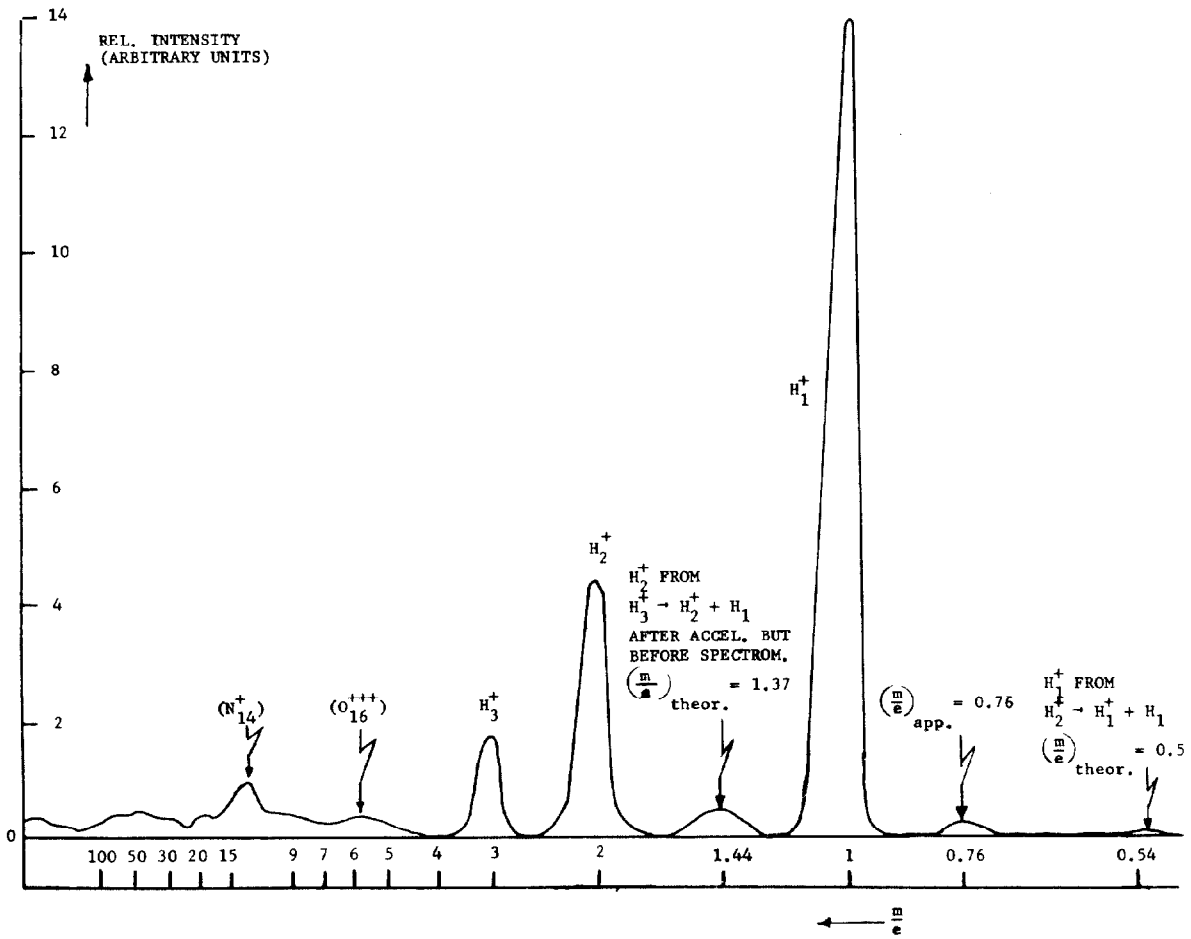

Fig. 2. Mass spectrum of 750 KeV beam from duoplasmatron source.

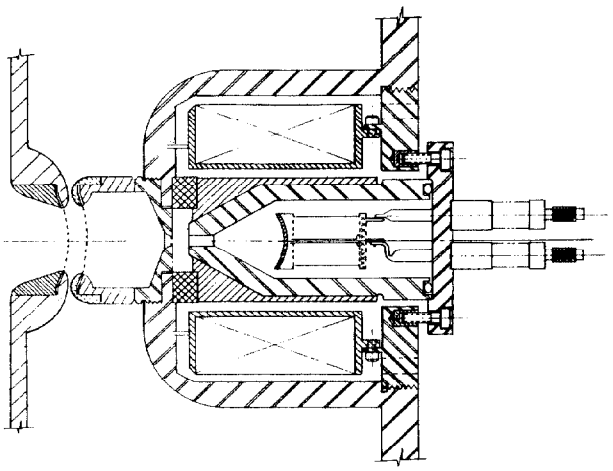

Fig. 3. Modified duoplasmatron.

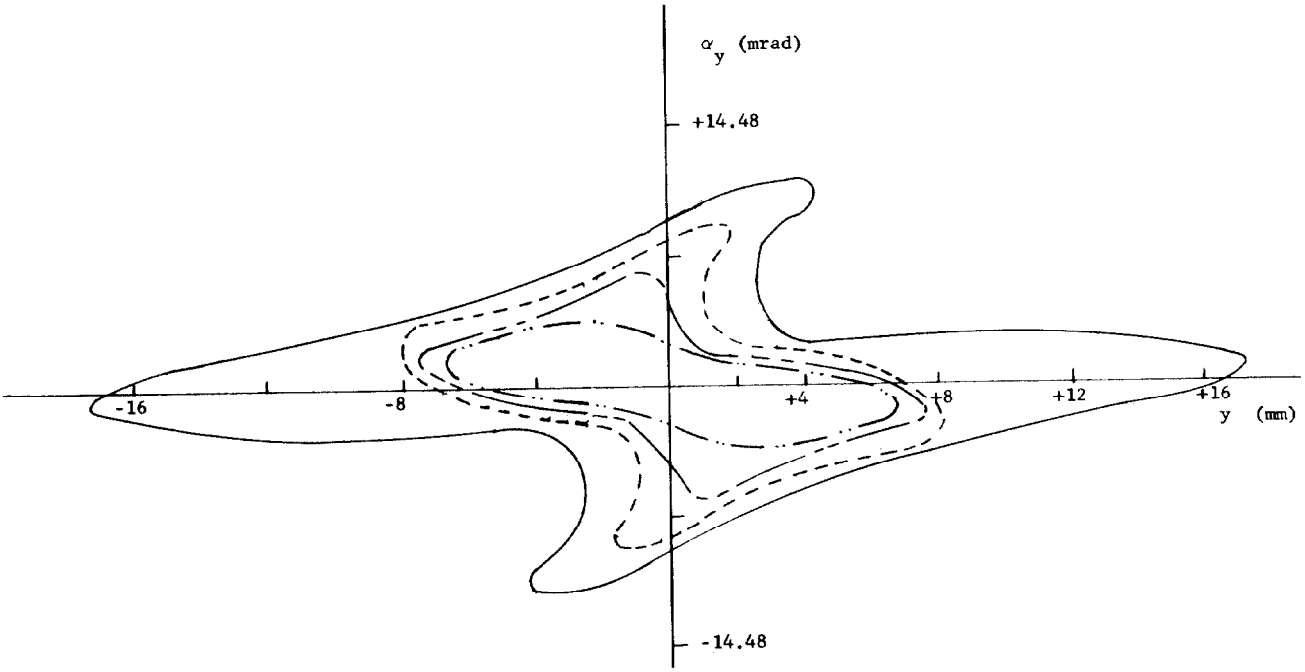

AREA $F(y, \alpha_y)_{750\ kev,\ 40\ ma}$

————	26.0 cm-mrad, 99% $I_{tot.}$
– – – – – –	12.3 - - , 91% -
—— · · ——	8.0 - - , 79% -
—— · · ——	5.0 - - , 65% -

Fig. 4. PIG Ion source emittance - 750 KeV.

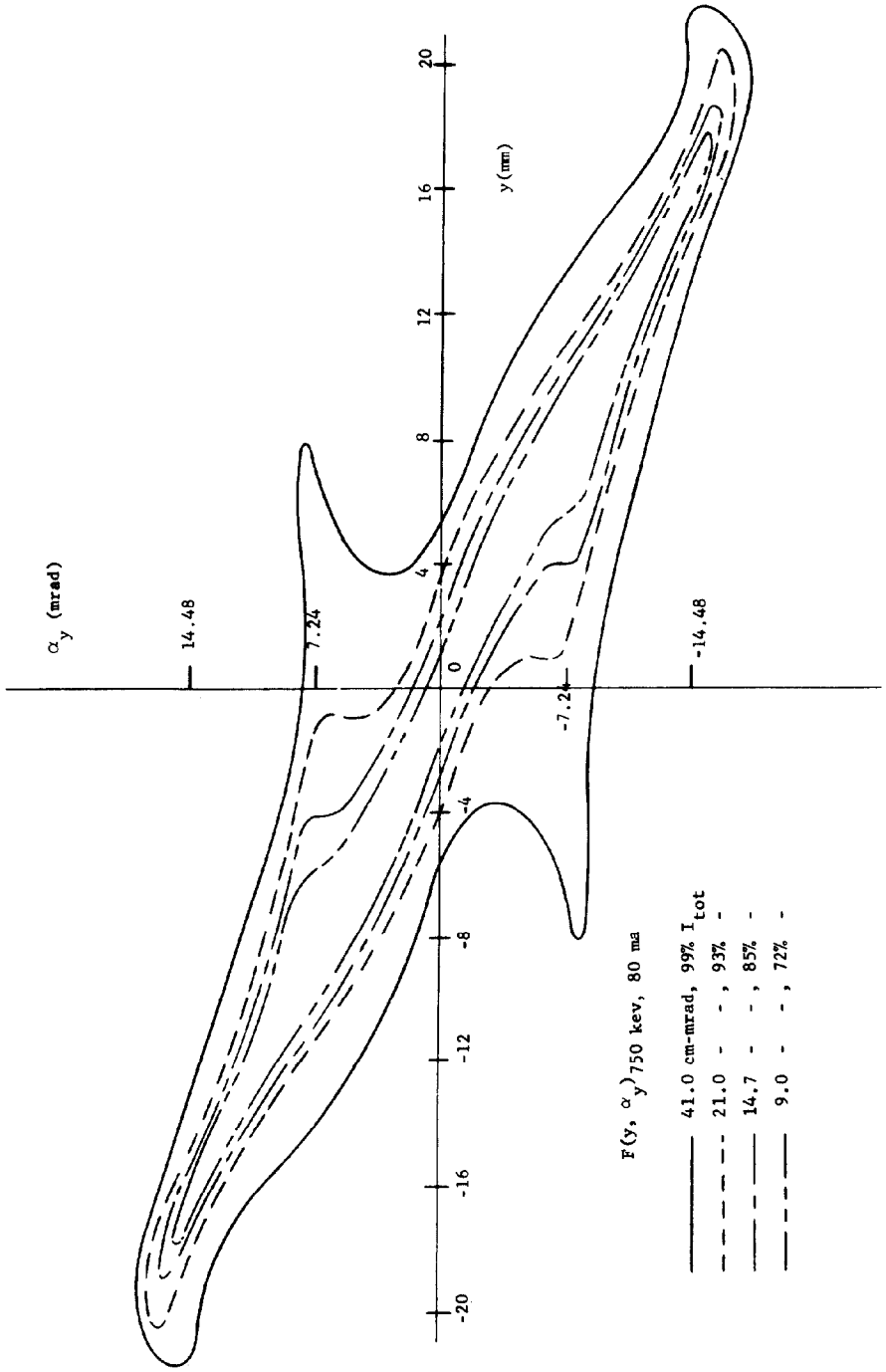

Fig. 5. Duoplasmatron source emittance - 750 KeV.

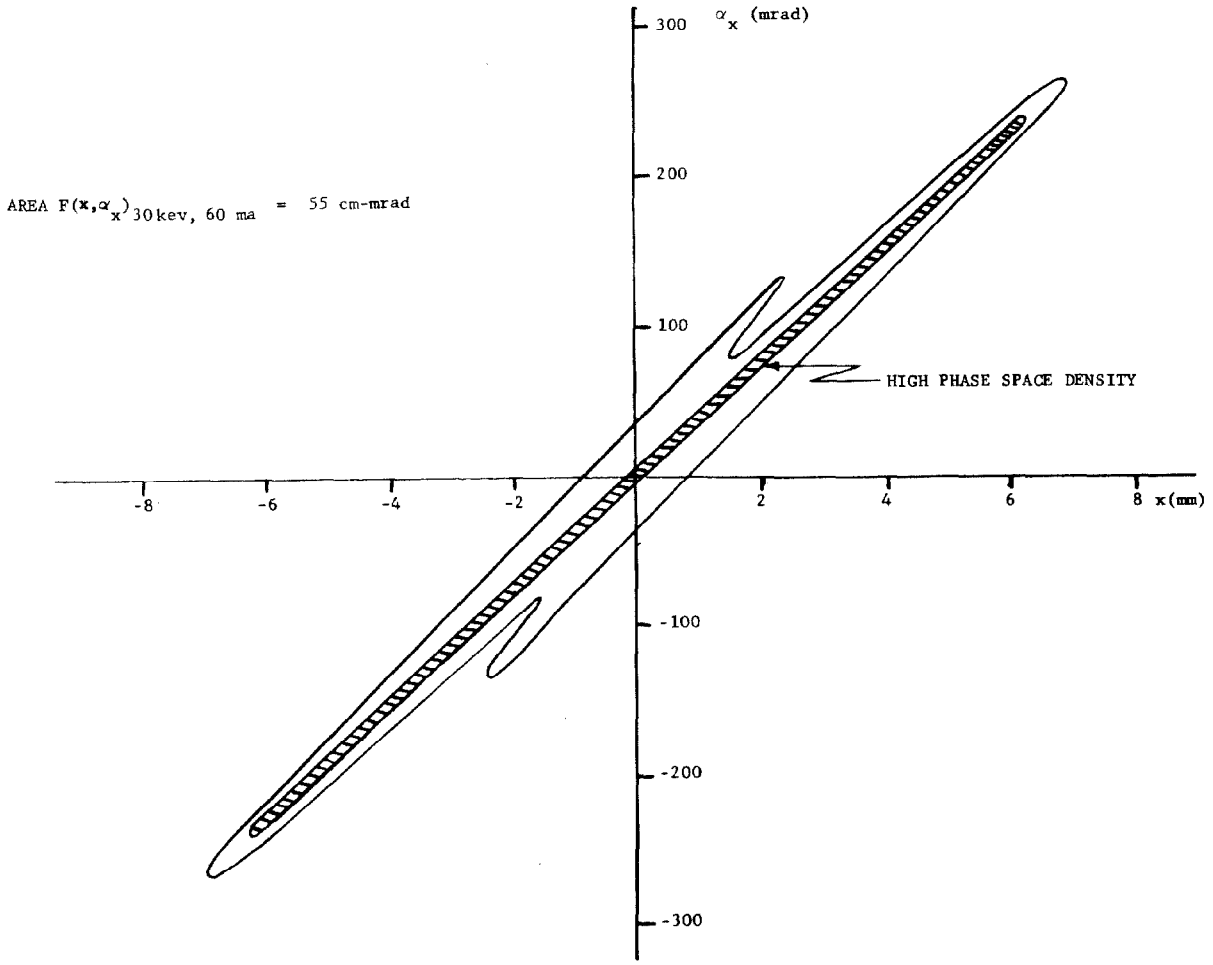

Fig. 6. Duoplasmatron source emittance - 30 KeV.

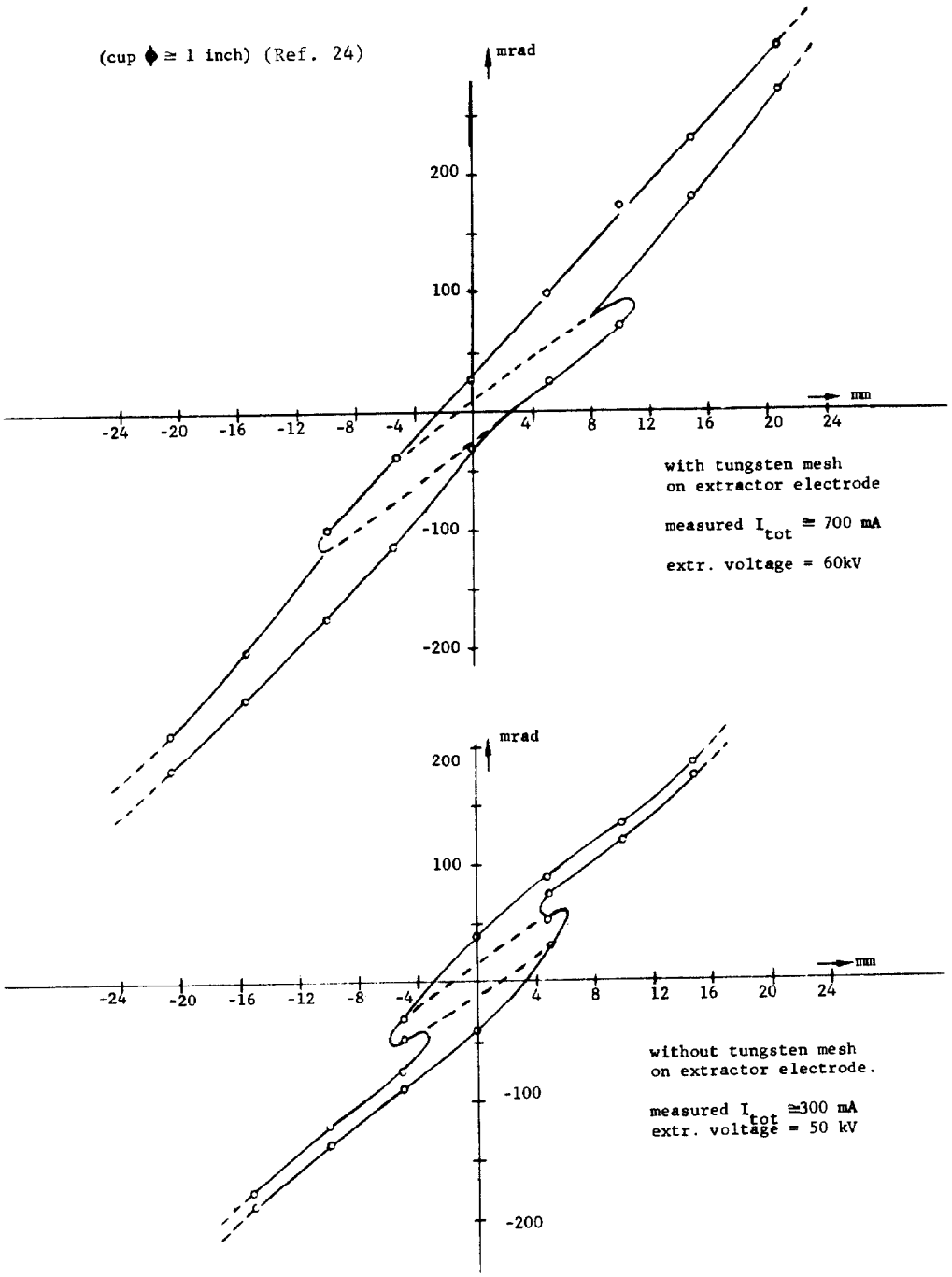

Fig. 7. Modified duoplasmatron source emittance - 50 KeV.

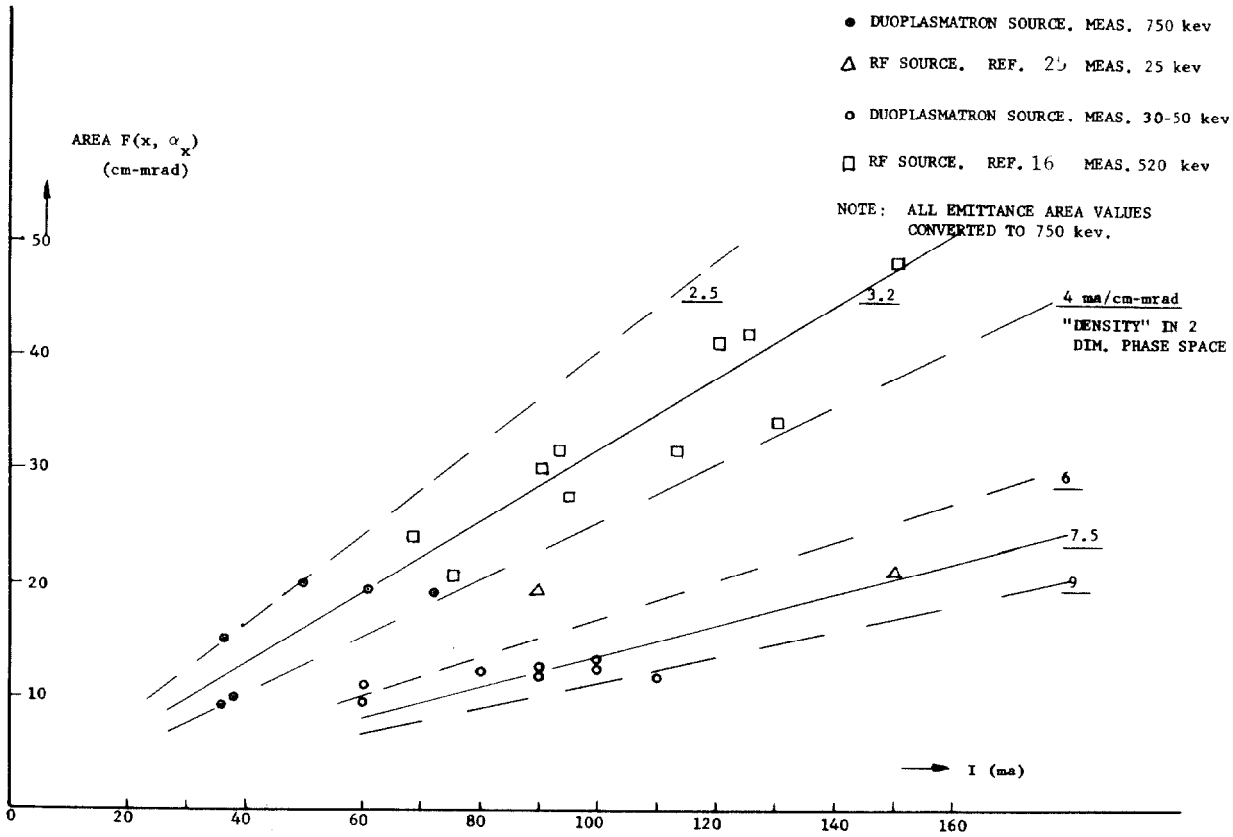

Fig. 8. Comparison duoplasmatron and rf source.

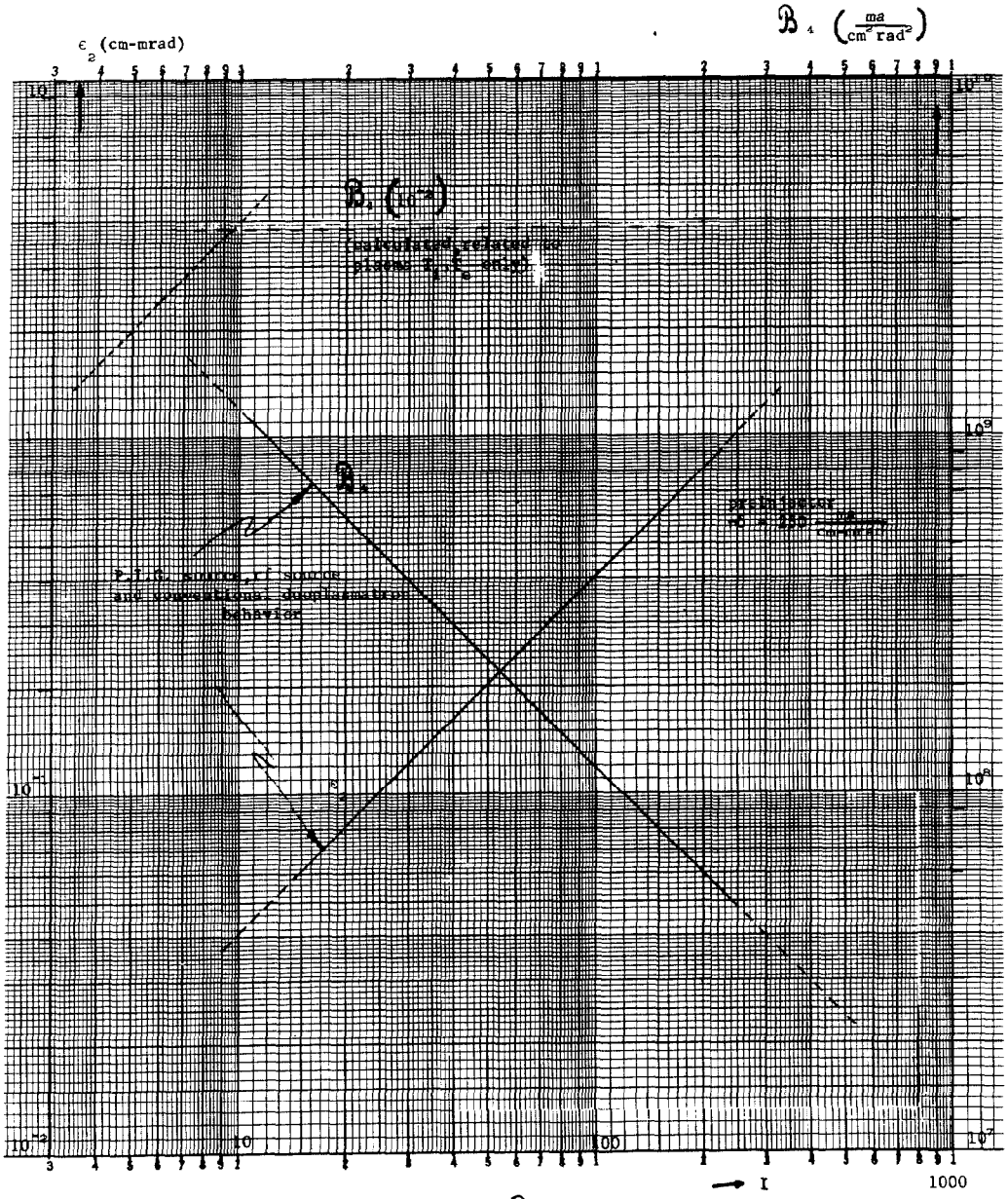

Fig. 9. $\epsilon_2 B_4$ versus I.

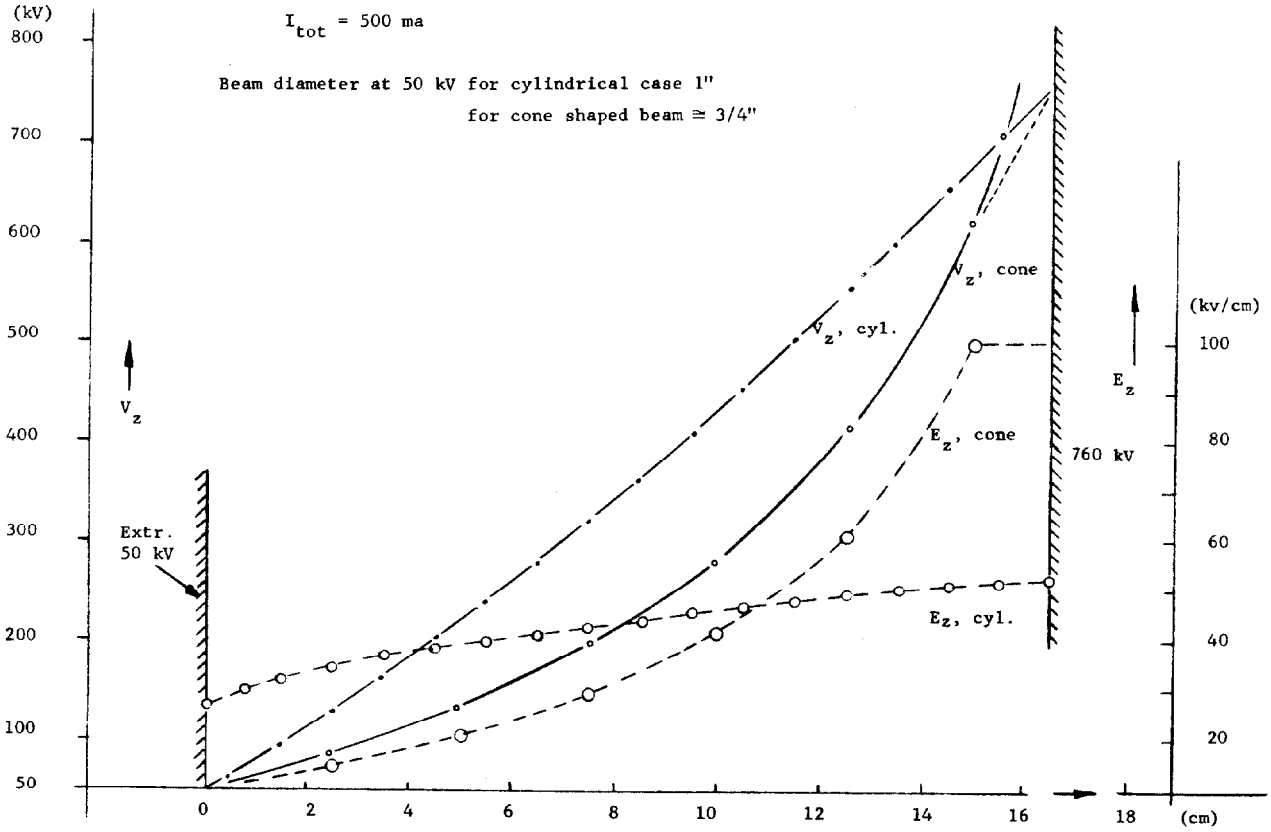

Fig. 10. High gradient beam design, axial potential distribution.

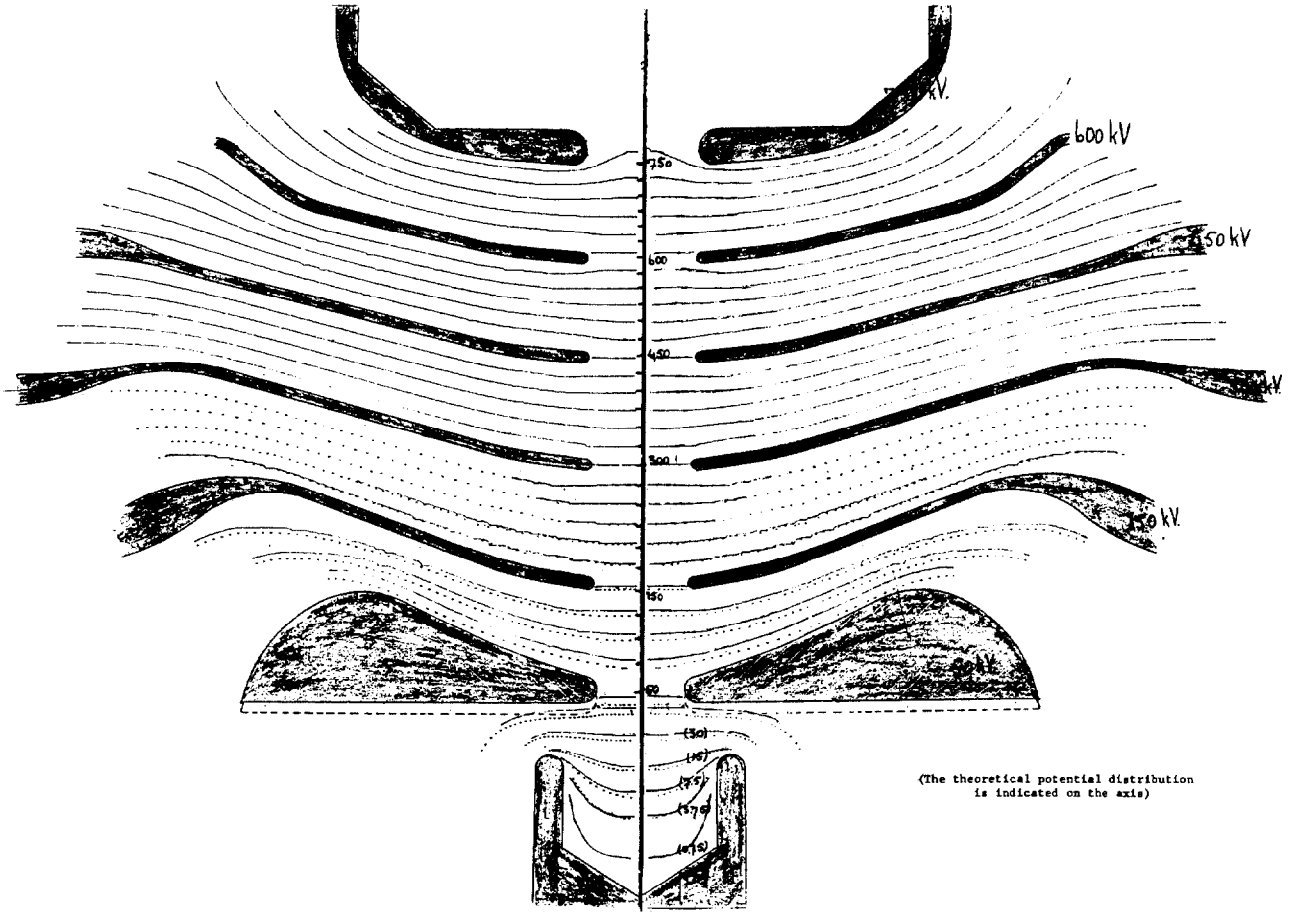

Fig. 11. High gradient beam design,
Equipotential distribution.

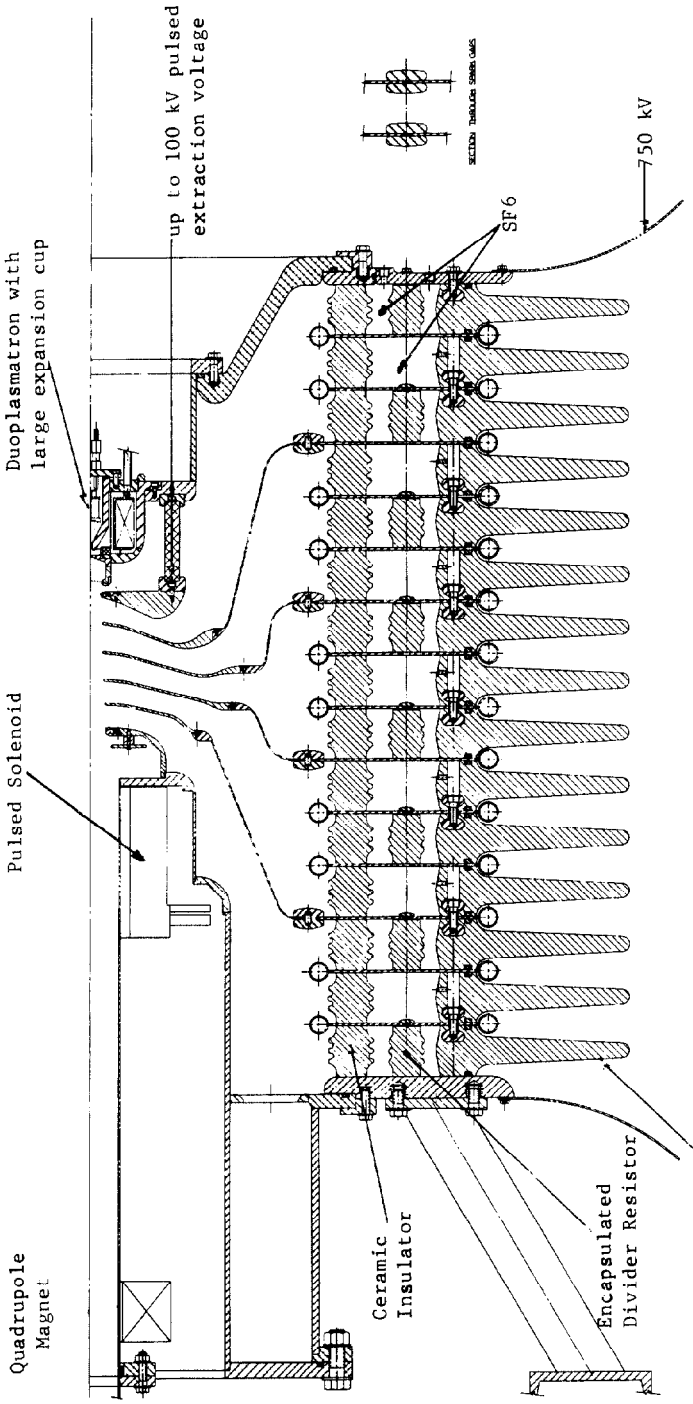

Fig. 12. High gradient accelerator column with modified duoplasmatron source.